

Single-particle positron potentials for a positron interacting with atoms

A. Zubiaga* and F. Tuomisto

*Department of Applied Physics, Aalto University,
P.O. Box 14100, FIN-00076 Aalto Espoo, Finland*

M. J. Puska

*COMP, Department of Applied Physics, Aalto University,
P.O. Box 11100, FIN-00076 Aalto Espoo, Finland*

Abstract

In this work we define single-particle potentials for a positron interacting with light atoms (H, He, Li and Be) by inverting a single-particle Schrödinger equation. For this purpose we use accurate energies and positron densities obtained from the many-body wavefunction of the corresponding positronic systems. The introduced potentials describe the exact non-adiabatic correlations for the calculated systems including the formation of a positronium atom in the e^+Li system. We show that the scattering lengths and the low energy s-wave phase shifts from accurate many-body calculations are well accounted for by the introduced potential. The two-component density-functional theory positron potentials for the bound e^+Li and e^+Be are in a very good agreement with the potentials introduced in this work, provided that the finite-positron-density electron-positron correlation potential is used. Also the density functional positron distributions agree surprisingly well with the many-body densities. The positron densities of the unbound e^+H and e^+He are not well described because the limit of the electron-positron energy functional derived from a homogeneous electron gas is not valid in the vacuum region. We argue that an effective potential can be used to calculate the positron distribution in molecular condensed matter when the inter-molecular interactions are weak, and the transferability of the potential is not of concern. We also address other concerns regarding the distinguishability of the Ps complex and the role of the accompanying electron in the positronium atom.

* asier.zubiaga@aalto.fi

I. INTRODUCTION

Although the chemistry of the positron in crystalline solids and soft-condensed matter has an intrinsic interest by itself, it is mainly studied in connection of probing the electron chemistry and the open volume of materials by positrons. Thermalized positrons become localized inside open volume defects such as vacancies and voids where the repulsion by the nucleus is minimum. Inside matter the annihilation occurs mainly through the fast pick-off quenching, during which typically two gamma photons are emitted. The annihilation properties of the positron are determined by the local electronic structures and the open volume distributions. The positron annihilation spectroscopy (PAS) allows to measure the size distributions and densities of vacancies in metals and semiconductors [1]. When probing soft matter, the positron chemistry has to be taken into account because a positron can bind an electron and form a positronium (Ps) complex before getting trapped into open volume pockets [2]. The distributions of open volume have been studied in porous SiO_2 [3, 4], polymers [5] and biostructures [6] by measuring the lifetime of Ps.

The interpretation of the PAS experimental data benefits of the comparison to computational predictions. The study of a positron embedded in a material requires a quantum-mechanical description of all the light particles, namely the electrons and the positron, to address the non-adiabatic correlations and the delocalization and the zero-point energy of the light particles. Regrettably, using many-body techniques for a full quantum-mechanical treatment of the interacting electron-positron system embedded in a host material is clearly beyond the present-day computational capacity. Instead, the density distributions and the annihilation properties of positrons in metals and semiconductors can be calculated from first principles to a good accuracy within the two-component density functional theory (2C-DFT) and the local density approximation (LDA) for the exchange and correlation functionals [7]. For a delocalized positron in a perfect lattice this scheme works well and the calculated positron annihilation parameters can be used for a quantitative analysis of the experimental results. Moreover, due to the screening effects, the same method can be applied also for positrons trapped at voids in metals and in semiconductors. However, this scheme is not able to describe Ps and instead semiempirical methods have been employed to describe the matter-Ps interaction [8].

The many-body wavefunctions of small positronic systems composed by a positron inter-

acting with a light atom or a small molecule can be calculated to a good accuracy using the Quantum Monte-Carlo (QMC) [9] and Configuration Interaction (CI) [10] methods. In this work we use accurate positron energies and densities obtained from a many-body exact diagonalization stochastic variational method (SVM) using the explicitly correlated Gaussian (ECG) function basis set. ECG-SVM accounts for more correlation energy than the other techniques for e^+Li [11] and e^+Be [12] and the resulting binding energies are the largest. We propose a single-particle potential for the positron which we derive for light positronic systems (e^+H , e^+He , e^+Li and e^+Be) inverting a single-particle Schrödinger equation.

We discuss the accuracy of the introduced potential comparing the scattering length and the s-wave phase shift to the many-body values. We also compare the many-body densities and the single-particle potential to the corresponding 2C-DFT values of e^+Li and e^+Be . Finally, we draw conclusions on the capability of the 2C-DFT and the introduced positron-atom potentials to describe positron and Ps states in condensed matter.

II. COMPUTATIONAL METHODS

A. ECG-SVM

ECG-SVM [13] is an all-particle quantum ab-initio method to calculate the many-body wavefunction which is an eigenstates of the non-relativistic Hamiltonian without the kinetic energy of the CM (T_{CM}), i.e.,

$$\hat{H} = \sum_i \frac{p_i^2}{2m_i} - T_{CM} + \sum_{i<j} \frac{q_i q_j}{4\pi\epsilon_0 r_{ij}}, \quad (1)$$

where \vec{p}_i is the momentum, m_i the mass, and q_i the charge of the i^{th} particle and r_{ij} is the distance between the i^{th} and j^{th} particles. The hadronic nucleus is treated as a point particle without structure, on equal footing with the electrons and the positron. The wavefunction is expanded in terms of a linear combination of properly antisymmetrized ECG functions,

$$\Psi(x) = \sum_{i=1}^s c_i \mathcal{A} \left[\exp^{-\frac{1}{2} x A^i x} \right] \otimes \chi_{SM_s}, \quad (2)$$

where A^i is the non-linear coefficient matrix and c_i the mixing coefficients of the eigenvectors. The antisymmetrization operator \mathcal{A} acts on the indistinguishable particles and χ_{SM_s} is a spin eigenfunction with $\hat{S}^2 \chi_{SM_s} = S(S+1)\hbar^2 \chi_{SM_s}$ and $\hat{S}_z \chi_{SM_s} = M_S \hbar \chi_{SM_s}$. The ECG use

Jacobi coordinate sets $\{x_1, \dots, x_{N-1}\}$ with the reduced mass $\mu_i = m_{i+1} \sum_{j=1}^i m_j / \sum_{j=1}^{i+1} m_j$ that allows for a straightforward separation of the CM movement. All the systems we have considered so far have zero total angular momentum, so we do not need to include spherical harmonics to describe the orbital motion. The many-body electron density is $n_-(r) = \sum_{i=1}^{N_e} \langle \Psi | \delta(\vec{r}_i - \vec{r}_N - \vec{r}) | \Psi \rangle$ and the positron density is $n_+(r) = \langle \Psi | \delta(\vec{r}_p - \vec{r}_N - \vec{r}) | \Psi \rangle$, where \vec{r}_i , \vec{r}_p , and \vec{r}_N are the coordinates of the i^{th} electron, the positron and the nucleus, respectively.

The ECG basis sets used in this work comprise between 200 and 2000 functions. Typically, systems with more particles need larger function basis sets for an accurate determination of the wavefunction. The non-linear coefficients $A_{\mu\nu}^i$ are to be optimized to avoid very large basis sets. SVM, which is better suited for functions with a large number of parameters than direct search methods, is used for this purpose. The values of the parameters are varied randomly and the new values are kept only if the update lowers the total energy of the system. The success of the ECG-SVM method relies on the efficient calculation of the matrix elements.

e^+Li and e^+Be are both large systems but e^+Be converges noticeably slower. We obtain 2.33×10^{-3} au for the positron binding energy, while the most accurate value from the literature is 3.163×10^{-3} au [12]. On the other hand, for e^+Li we obtain 2.42×10^{-3} au for its dissociation energy against Li^+ and Ps and the largest value, also using ECG-SVM [11], is 2.4821×10^{-3} au.

Unbound e^+H and e^+He cannot be calculated without adding a confining potential. We used a weak two-body attractive potential,

$$V(r_p) = \begin{cases} 0 & , \quad r < R_0 \\ \alpha(r_p - R_0)^2 & , \quad r \geq R_0, \end{cases} \quad (3)$$

binding the positron to the hadronic nucleus in a similar fashion to the confinement potential used by Mitroy et al. to describe positrons scattering off atoms [14]. The potential is different from zero only when the nucleus-positron distance r_p grows above a boundary value R_0 , and then it has a parabolic increase. R_0 and α were set so that the average nucleus positron distance $\langle r_p \rangle \gtrsim 50$ au. The variational procedure explained above can be used also to optimize the basis set of the confined system also. The confinement radius is chosen large enough (100 au) so that the shape of the wavefunction is not affected in the interaction

Table I. Main properties of the positronic systems. The first four columns give the name of the system, the size of the basis used, the total energy, and the $\langle r_p \rangle$. The next three columns give the asymptotic state, the total energy of the corresponding atom or ion and the interaction energy.

System	Basis size	Energy (au)	$\langle r_p \rangle$ (au)	Asymptotic state	Atom/Ion Energy (au)	$E_{int}^{e+}/E_{int}^{Ps}$ (au)
e^+H	200	-0.49974	67.47	e^+	-0.5 (H)	0.262×10^{-3}
e^+He	1000	-2.90332	56.98	e^+	-2.9036937 (He)	0.372×10^{-3}
e^+Li	1000	-7.53226	9.928	Ps	-7.4779733 (Li) -7.2798377 (Li^+)	-2.42×10^{-3}
e^+Be	2000	-14.6694	10.972	e^+	-14.6670283 (Be) -14.3246131 (Be^+)	-2.33×10^{-3}

region by the confinement potential. The resulting $\langle r_p \rangle$ is large and the interaction energy is small.

For unbound e^+H and e^+He the asymptotic state of the interacting system, when the positron is far from the atom, is the main scattering channel, i.e., the positron scatters off the neutral atom, and for bound e^+Li and e^+Be it is the main dissociation channel. While e^+Be splits into a neutral atom and a positron, e^+Li splits into a Li^+ ion and a Ps atom.

We call to the difference between the energy of the interacting system, E_{Xe^+} , and the isolated atom, E_X , the positron interaction energy $E_{int}^{e+} = E_{Xe^+} - E_X$ and to the difference between E_{Xe^+} and the sum of the total energies of the positive ion, E_{X^+} , and Ps, E_{Ps} the Ps interaction energy, $E_{int}^{Ps} = E_{Xe^+} - E_{X^+} - E_{Ps}$.

B. Two-component DFT

Within the LDA of the 2C-DFT the energy of the positronic atoms is

$$\begin{aligned}
 E[n_-(r), n_+(r)] = \\
 F_1[n_-] + F_2[n_+] + E_C^{ep}[n_-, n_+] + E_{corr}^{ep}[n_-, n_+],
 \end{aligned} \tag{4}$$

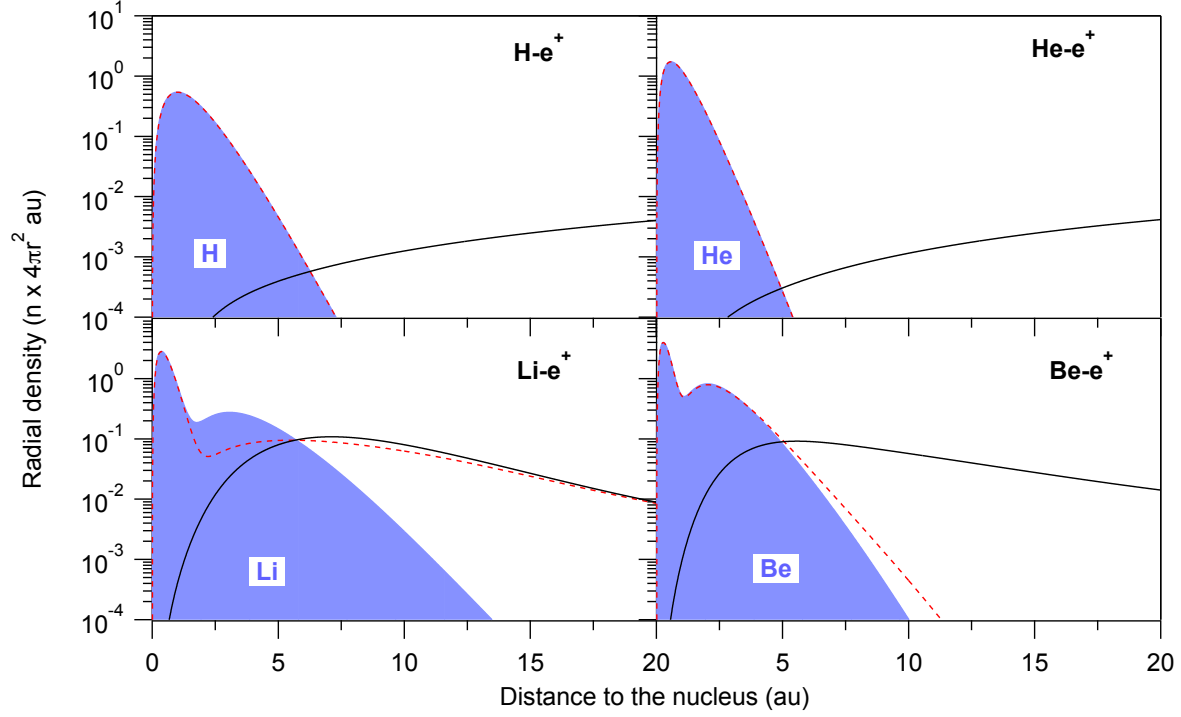


Figure 1. (Color online) Electron and positron densities of e^+H , e^+He , e^+Li , and e^+Be . The electron densities of the isolated atoms (filled blue curve), and the interacting positron-atom systems (red broken curve), as well as the positron density (black full curve) are given.

where $E_C^{ep}[n_-, n_+]$ is the attractive Coulomb interaction between the electrons and the positron and $E_{corr}^{ep}[n_-, n_+]$ is the electron-positron correlation energy. $F_1[n]$ is the usual one-component density functional

$$F_1[n] = E_{kin}[n] + E_{ext}[n] + E_H[n] + E_{xc}[n], \quad (5)$$

where $E_{ext}[n]$, $E_H[n]$, and $E_{xc}[n]$ are the electron(positron)-nucleus interaction, the Hartree energy functional and the exchange-correlation energy functional parametrized by Perdew and Zunger [15], respectively. $E_{kin}[n]$ is the Kohn-Sham kinetic energy. The self-interaction corrected (SIC) density functional for a single positron $F_2[n]$ is

$$F_2[n] = E_{kin}[n] + E_{ext}[n]. \quad (6)$$

The asymmetric treatment of the electron and positron self-interactions for positron states in solids has been shown to give results in a quantitative agreement with experiments [16, 17].

The resulting Kohn-Sham equations for the electron ϕ_i^- and positron ϕ^+ orbitals are

$$\left[-\frac{\nabla^2}{2} - \frac{Z}{r} + \int \frac{n_-(x) - n_+(x)}{|\vec{r} - \vec{x}|} d\vec{x} + \frac{\delta E_{xc}[n_-]}{\delta n_-} + \frac{\delta E_{corr}^{ep}[n_+, n_-]}{\delta n_-} \right] \phi_i^- = \epsilon_i^- \phi_i^- \quad (7)$$

$$\left[-\frac{\nabla^2}{2} + \frac{Z}{r} - \int \frac{n_-(x)}{|\vec{r} - \vec{x}|} d\vec{x} + \frac{\delta E_{corr}^{ep}[n_+, n_-]}{\delta n_+} \right] \phi^+ = \epsilon^+ \phi^+, \quad (8)$$

where Z is the atomic number of the nucleus and ϵ_i^- and ϵ^+ are the electron and positron energy eigenvalues, respectively. Equations 7 and 8 are solved self-consistently with a modified DFT program for the electronic structures of free atoms [18].

To build the electron positron correlation energy functional $E_{ep}[n_+, n_-]$ we use the correlation energies calculated by Lantto [19] for a homogeneous electron-positron plasma in the metallic regime. $E_{ep}[n_+, n_-]$ is symmetric in the electron and the positron densities and we require, following reference [17], that at the limit of the vanishing positron density the energy of a single positron in a homogeneous electron gas is obtained [20].

III. RESULTS

The ionization energies of H and He are 0.5 au and 0.90369 au, respectively, well above the binding energy of Ps (0.25 au) and the electrons, see figure 1, remain tightly bound to the nuclei without an appreciable polarization. The positrons are completely delocalized and only a small fraction of the density enters the electron cloud of the atom. The ionization energy, 0.34242 au, of the closed 2s orbital of Be is slightly larger than the Ps binding energy so that the electrons get slightly polarized and the positron becomes bound by the induced dipole. On the other hand, the Li ionization energy of 0.198 au is lower than the binding energy of Ps and the positron forms a Ps cluster with the 2s electron [21].

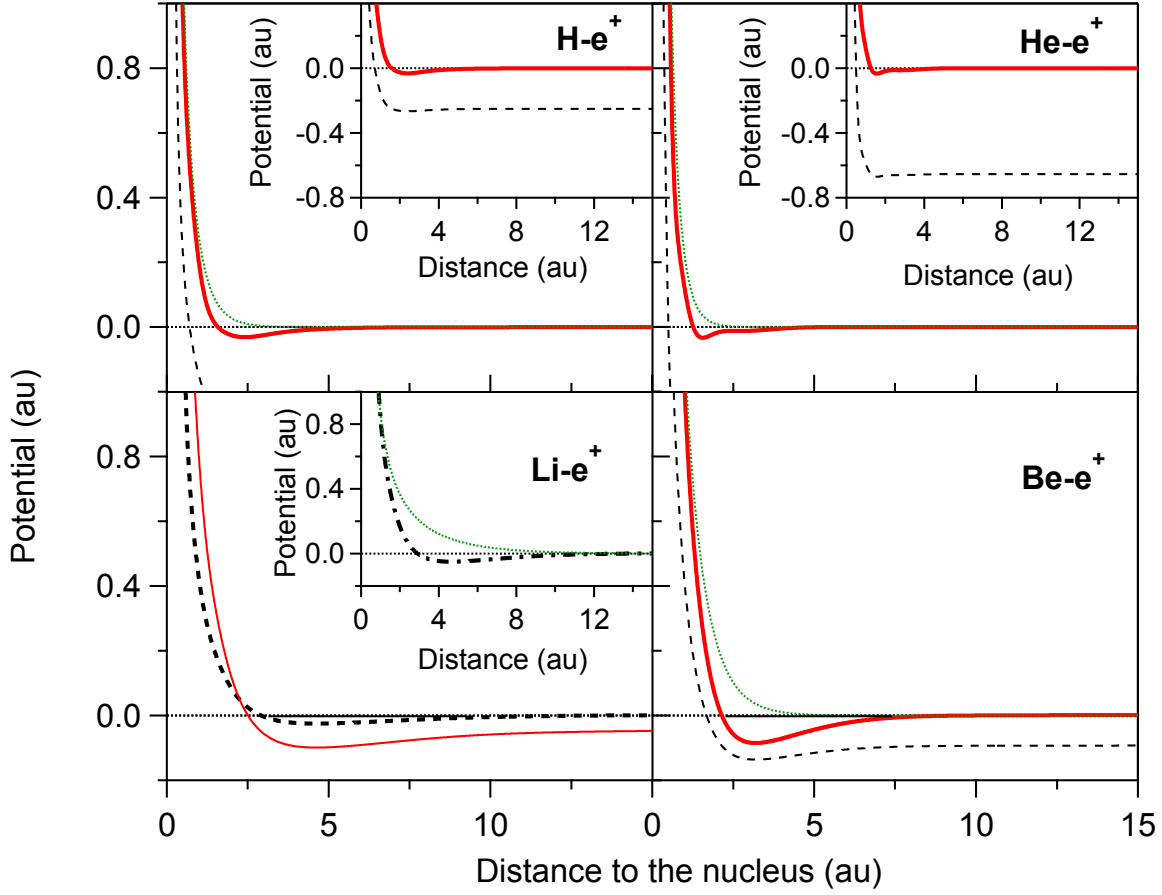


Figure 2. (Color online) V_{eff} and the positron Coulomb potentials for e^+H (upper left), e^+He (upper right) and e^+Be (lower right) and the Ps V_{eff} potential for e^+Li (lower left). The Ps V_{eff} potentials are plotted with black dashed lines, the positron V_{eff} potentials with red full lines and the positron Coulomb potentials with green dotted lines. The inset in the panel of e^+Li compares the mass-normalized Ps V_{eff} (black dash-dotted line) and its Coulomb potential.

A. Effective potentials

We invert a single particle Schrödinger equation using the positron densities of the interacting systems to obtain an effective potential

$$V_{eff}(r) = E_{eff} + \frac{1}{2M_{eff}} \frac{\nabla^2 \sqrt{n_+(r)}}{\sqrt{n_+(r)}}. \quad (9)$$

The effective energy E_{eff} and the effective mass M_{eff} are the interaction energy and the mass of the positron or Ps in the asymptotic state, respectively. The E_{eff} values are those

of E_{int} in table I. The effective mass M_{eff} is the mass of the Ps ($2m_e$) for e^+Li and the mass of the positron (m_e) for e^+H , e^+He , and e^+Be .

Figure 2 shows that only for the E_{eff} and M_{eff} of the asymptotic state, V_{eff} is zero when the positron is far from the nucleus. We also define a mass-normalized Ps effective potential $V_{eff'}^{Ps} = 2E_{int}^{Ps} + \nabla^2(\sqrt{n_+})/(2\sqrt{n_+})$ with the effective mass m_e . The densities obtained solving the Schrödinger equation with the mass normalized potential are the same as those of V_{eff} and the energies are multiplied by a factor of 2. In the present work, we use the mass-normalized potential to compare the V_{eff} of e^+Li to the positron DFT potentials.

According to figure 2, when $r \lesssim 1$ au the positron-nucleus Coulomb repulsion dominates over the electron-positron attractive Coulomb and correlation potentials. For larger separations the electron-positron correlation is comparable to the Coulomb repulsion and V_{eff} becomes attractive. The positron V_{eff} of the unbound e^+H and e^+He have a strongly repulsive core for $r \lesssim 1.2$ au. For the e^+Li and e^+Be the core region extends further until $\sim 2-3$ au because the 2s electrons are more delocalized. The attractive well of the unbound states is shallow and it extends until ~ 5 au. Due to the larger polarizability of H, the attractive well is slightly deeper for e^+H than for e^+He . The minimum value of the binding potential well of e^+Li is -24.57×10^{-3} au at a separation of 4.62 au. Finally, the potential well of e^+Be is rather deep, -84.58×10^{-3} au at 3.18 au.

To check that V_{eff} can predict the correct positron density and interaction energy, we have calculated the positron (Ps) binding energy to Be (Li^+) by solving numerically the radial single-particle Schrödinger equation. For the ground state it reduces to the one-dimension problem

$$-\frac{1}{2M_{eff}} \frac{d^2U}{dr^2} + V_{eff}U = EU, \quad (10)$$

where $U = r\Psi$ and Ψ is the s-type wavefunction. The boundary conditions for U are $U(r=0)=0$ and $U(r \rightarrow \infty)=0$. The binding energy and $\langle r_p \rangle$ given by equation 10 are, $E_b = 2.414 \times 10^{-3}$ au and $\langle r_p \rangle = 10.213$ au for e^+Li and $E_b = 2.33 \times 10^{-3}$ au and $\langle r_p \rangle = 11.104$ au for e^+Be , in good agreement with the values obtained from the corresponding many-body wavefunctions.

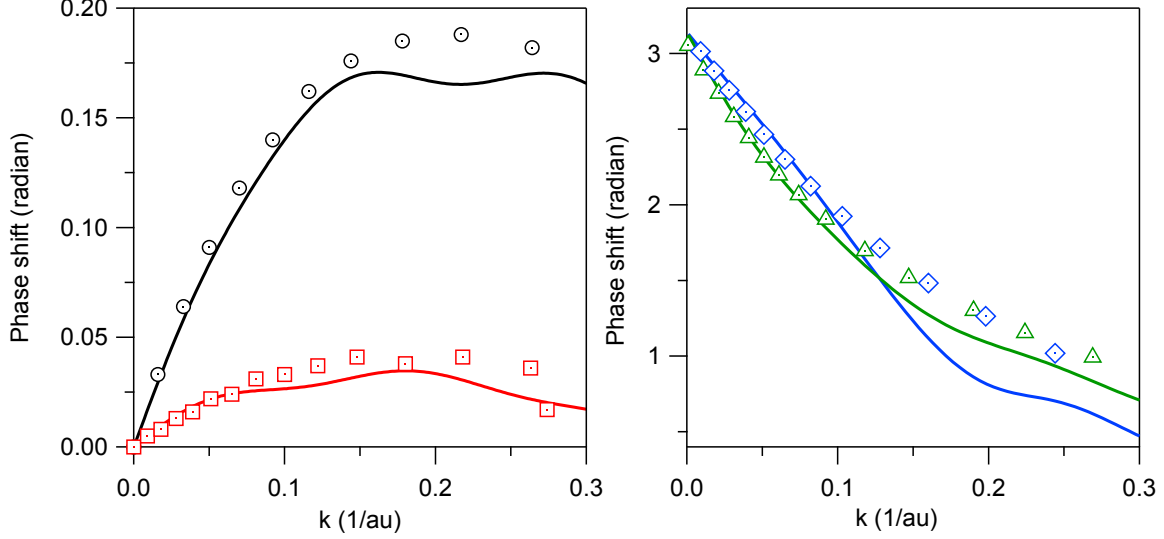


Figure 3. (Color online) s-wave phase shifts for positrons scattering off H (black line), He (red line), Li (blue line) and Be (green line). The many-body values obtained by Zhang et al. [22] for H (black dotted circles), He (red dotted squares) and Li (blue dotted diamonds) and Bromley et al. [24] for Be (green dotted triangles) are also shown.

B. Scattering Lengths

Many-body calculations of the s-wave phase shifts (δ_0) and scattering lengths (a_0) exist for the systems studied. Zhang et al. [22] used the stabilized ECG-SVM to calculate the positron a_0 of H and He and the Ps a_0 of Li^+ . Houston et al. [23] applied Hylleraas wavefunctions and the Kohn variational method to positrons scattering off H and Bromley et al. [24] studied positron scattering off Be using polarized orbital wavefunctions.

Here we calculate δ_0 and a_0 using V_{eff} and compare them to the many-body values of the literature. For a positron scattering off Li, the polarization of the target atom and the formation of Ps are important already at low energies [25] and therefore the V_{eff} values of e^+Li are compared to the Ps scattering length and δ_0 of Li^+ , instead. We obtain the s-wave scattering wavefunction for a positron of the energy $E = k^2/2M_{eff}$ and mass M_{eff} by solving equation 10. At large distances from the nucleus the wavefunction has the form

$$\lim_{r \rightarrow \infty} \psi_0 = \frac{\sin(kr + \delta_0)}{kr}. \quad (11)$$

The wavefunction calculated numerically is fitted to this asymptote to obtain δ_0 as a function

of k . a_0 is then calculated at the low-energy limit from $k \cot \delta_0 = -1/a_0 + O(k^2)$.

Table II. Positron scattering lengths computed using V_{eff} . The values in the last column are from many-body calculations of the literature. All the values are given in au.

e^+H	-1.86	-2.094 [22], -2.10278 [23]
e^+He	-0.55	-0.474 [22]
e^+Be	18.76	16 [24]
Ps-Li ⁺	12.19	12.9 [22]

The calculated δ_0 are plotted in figure 3. They show good agreement with the many-body values for $k \lesssim 0.1 \text{ au}^{-1}$ what suggests that V_{eff} will remain valid to describe quasi-thermalized positrons at room temperature. For larger momenta the dynamical correlation becomes important and our values are systematically slightly lower. For Ps scattering off Li⁺ the difference is the largest, 0.3-0.4 radians, because both the target and the projectile are deformed. For a positron scattering off Be the agreement is very good considering that the many-body wavefunction of e^+Be is not well optimized and the binding energy calculated from V_{eff} is smaller than in the many-body calculation.

The scattering lengths calculated using V_{eff} , shown in table II, are comparable to the many-body values for H, He and Li. The large difference for Be reflects that in our calculation the positron binding energy to Be is 0.8×10^{-3} smaller (26%) than the best many-body value [12] and 0.5×10^{-3} smaller (16%) than the binding energy by Bromley et al.

C. Two-component DFT: e^+Li and e^+Be

In the following we will focus in self-consistent 2C-DFT calculation of the bound e^+Li and e^+Be . H and He atoms have large polarizability within LDA-DFT and the self-consistent 2C-DFT predicts the formation of shallow bound states for both positronic systems. The positron density extends to the vacuum where the electron-positron correlation energy limit parametrized from a homogeneous electron gas is not valid. Figure 4 compares the radial electron and positron densities of both systems calculated with 2C-DFT to our ECG-SVM results. The vanishing positron-density limit [20] of the electron-positron correlation potential doesn't predict the formation of bound states, and the 2C-DFT densities are obtained

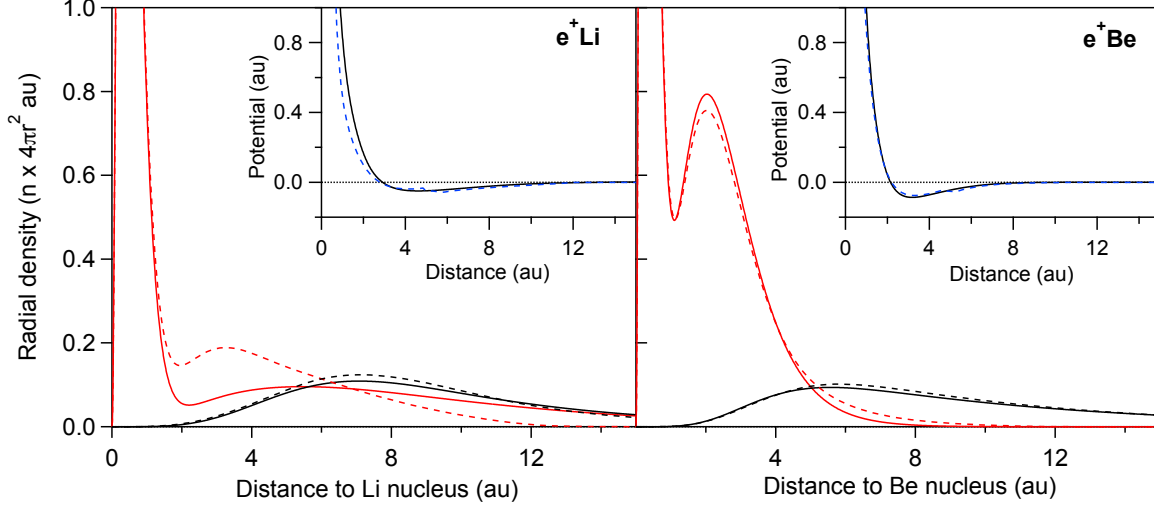


Figure 4. (Color online) Electron (red line) and positron (black line) radial ECG-SVM (full lines) and 2C-DFT (broken lines) densities. The insets show the V_{eff} potential (black full line) and positron 2C-DFT potential (blue dashed line) for e^+Li (left panel) and e^+Be (right panel). For e^+Li the mass normalized potential has been plotted.

using the positron-density dependent LDA electron-positron correlation potential instead. The 2C-DFT positron density of e^+Be matches the many-body density whereas the 2C-DFT electron density is slightly more delocalized than the many-body density. The 2C-DFT positron density of e^+Li is also close to the many-body result. However, according to 2C-DFT the electrons are more tightly bound to the nucleus than in the many-body calculation. The attraction wells of the 2C-DFT positron potentials match the V_{eff} in both systems. Only close to the Li nucleus the 2C-DFT positron potential is less repulsive than V_{eff} . However, the effect on the positron density is minor.

The 2C-DFT densities of e^+Li don't show the formation of Ps. The asymmetric behavior of the 2C-DFT electron and positron densities with respect to the many-body calculations reflects the means of DFT to describe correlations in the interacting many-body system [26]. The lack of SIC for the electrons causes the 2s orbital of e^+Li to be poorly described with DFT. Also, the binding energies of the positrons are only qualitative, reflecting the general inadequacy of LDA to accurately describe binding between atoms. Moreover, it is a well known problem that DFT within LDA is not able to describe dispersion interactions [27]. However, figure 4 shows convincingly that the electron-positron correlation potential derived

from the energy of an electron-positron plasma in the metallic regime yields accurate positron densities in bound positronic atoms, including the cases when Ps forms.

IV. V_{eff} FOR POSITRON AND Ps STATES IN CONDENSED MATTER

The trapping of positrons in vacancies inside metals and semiconductors occurs because the positron-nucleus repulsion is minimum. In addition, the valence electrons partly relax into the vacancy as attracted by the positron what increases the binding energy and the degree of localization of the positron.

The vanishing positron density limit of the electron-positron correlation energy within the 2C-DFT [17] yields reliable densities for positrons trapped at vacancies. To simplify the calculations or to compare different approaches, it would be desirable to calculate the positron potentials as atomic superpositions of V_{eff} in condensed matter also. However, the transferability of V_{eff} deduced from single positronic atoms or molecules is of concern. V_{eff} assumes that the valence electrons remain bound to the atoms and its atomic superposition cannot predict the trapping in vacancies in metals and semiconductors. The usability of V_{eff} will be limited to condensed matter systems where the electronic structures of the constituent atoms or molecules remain nearly undisturbed. This is the case in molecular soft condensed matter and in liquids where the inter-molecular interactions are weak. In these materials the superposition of molecular V_{eff} potentials can be a useful description for the positron state. The superposition of molecular V_{eff} potentials is specially interesting to study Ps embedded in molecular materials like polymers, liquids or biostructures.

The derivation of V_{eff} requires high quality positron densities obtained from quantum many-body techniques. This method is computationally demanding for large molecules with the present computing capacity but smaller systems like Ps-He can be studied [28], instead. He does not bind Ps due to its closed shell structure and low polarizability and it provides a good model system to study the interaction of Ps with molecular matter.

V. CONCLUSIONS

We have calculated the ECG-SVM many-body wavefunction for several positronic systems involving light atoms (H, He, Li and Be). Based on these results we have proposed an

effective single-particle positron potential by inverting the single-particle Schrödinger equation arising from the many-body positron density. V_{eff} is a single-particle potential for the positron and for Ps and it includes the full many-body correlations. It gives the correct binding energies and the positron densities of the bound states. The positron scattering lengths and the s-wave phase shifts are consistent with the many-body values of the literature.

We have shown that the low-energy correlations are well described by V_{eff} up to energies larger than that of quasi-thermalized positrons and Ps at room temperature. V_{eff} can be used to calculate the positron distribution in molecular condensed matter when the inter-molecular interactions are weak, i.e., when the transferability is not of concern. The success of V_{eff} to describe the positron in e^+Li , where a Ps complex forms, suggests that the potential can be also a valid single-particle description for the low-energy (quasi-thermalized) positron forming Ps without solving the Schrödinger equation for the many-body system. This possibility should be further studied in connection with Ps interacting with molecular systems.

We have shown the positron densities are well described with the 2C-DFT for bound e^+Li and e^+Be when the finite positron-density functional is used for the electron-positron correlation energy. The self-consistent 2C-DFT positron potentials predict the binding potential well of V_{eff} accurately. Although 2C-DFT within LDA yields inaccurate electron densities, our results indicate that 2C-DFT can be used to describe positrons in finite systems, including those in which Ps is formed. This result opens the possibility to use 2C-DFT also to describe Ps interacting with extended systems.

ACKNOWLEDGMENTS

This work was supported by the Academy of Finland through the individual fellowships and the centre of excellence program. We acknowledge the computational resources provided by Aalto Science-IT project. Thanks are due to K. Varga for providing us the ECG-SVM code used in this work.

[1] F. Tuomisto and I. Makkonen, Rev. Mod. Phys. **85**, 1583 (2013).

- [2] O. E. Mogensen, in *Positron Annihilation in Chemistry*, Springer Series in Chemical Physics, Vol. 58, edited by H. K. V. Lotsch (Springer-Verlag, 1995).
- [3] Y. Nagai, Y. Nagashima, and T. Hyodo, *Phys. Rev. B* **60**, 7677 (1999).
- [4] L. Liskay, C. Corbel, P. Perez, P. Desgardin, M.-F. Barthe, T. Ohdaira, R. Suzuki, P. Crivelli, U. Gendotti, A. Rubbia, M. Etienne, and A. Walcarius, *Appl. Phys. Lett.* **92**, 063114 (2008).
- [5] A. Uedono, R. Suzuki, T. Ohdaira, T. Uozumi, M. Ban, M. Kyoto, S. Tanigawa, and T. Mikado, *J. Polym. Sci. Part B* **36**, 2597 (1998).
- [6] P. Sane, E. Salonen, E. Falck, J. Repakova, F. Tuomisto, J. Holopainen, and I. Vattulainen, *J. Phys. Chem. B letters* **113**, 1810 (2009).
- [7] M. J. Puska and R. M. Nieminen, *Rev. Mod. Phys.* **66**, 841 (1994).
- [8] S. J. Tao, *J. Chem. Phys.* **56**, 5499 (1972); M. Eldrup, D. Lightbody, and J. N. Sherwood, *Chem. Phys.* **63**, 51 (1981); H. Schmitz and F. Müller-Plathe, *J. Chem. Phys.* **112**, 1040 (2000).
- [9] Y. Kita, R. Maezono, M. Tachikawa, M. Towler, and R. J. Needs, *J. Chem. Phys.* **131**, 134310 (2009); **135**, 054108 (2011); D. Bressanini, M. Mella, and G. Morosi, **108**, 4756 (1997); **109**, 1716 (1998); **109**, 5931 (1998); M. Mella, G. Morosi, D. Bressanini, and S. Elli, **113**, 6154 (2000).
- [10] R. J. Buenker and H. P. Liebermann, *J. Chem. Phys.* **131**, 114107 (2009).
- [11] J. Mitroy, *Phys. Rev. A* **70**, 024502 (2004).
- [12] J. Mitroy, *J. At. Mol. Sci.* **1**, 275 (2010).
- [13] K. Varga and Y. Suzuki, *Phys. Rev. C* **52**, 2885 (1995).
- [14] J. Mitroy, J. Y. Zhang, and K. Varga, *Phys. Rev. Lett.* **101**, 123201 (2008).
- [15] J. P. Perdew and A. Zunger, *Phys. Rev. B* **23**, 5048 (1981).
- [16] E. Boroński and R. M. Nieminen, *Phys. Rev. B* **34**, 3820 (1986).
- [17] M. J. Puska, A. P. Seitsonen, and R. M. Nieminen, *Phys. Rev. B* **52**, 10947 (1995).
- [18] P. Giannozzi, S. Baroni, N. Bonini, M. Calandra, R. Car, C. Cavazzoni, D. Ceresoli, G. L. Chiarotti, M. Cococcioni, I. Dabo, A. Dal Corso, S. de Gironcoli, S. Fabris, G. Fratesi, R. Gebauer, U. Gerstmann, C. Gougoussis, A. Kokalj, M. Lazzeri, L. Martin-Samos, N. Marzari, F. Mauri, R. Mazzarello, S. Paolini, A. Pasquarello, L. Paulatto, C. Sbraccia, S. Scandolo, G. Sclauzero, A. P. Seitsonen, A. Smogunov, P. Umari, and R. M. Wentzcovitch, *Journal of Physics: Condensed Matter* **21**, 395502 (2009).

- [19] L. J. Lantto, Phys. Rev. B **36**, 5160 (1987).
- [20] J. Arponen and E. Pajanne, Ann. Phys. **121**, 343 (1978); N. D. Drummond, P. L. Rios, R. J. Needs, and C. J. Pickard, Phys. Rev. Lett. **107**, 207402 (2011).
- [21] J. Mitroy, M. W. J. Bromley, and G. G. Ryzhikh, J. Phys. B: At. Mol. Opt. Phys. **35**, R81 (2002).
- [22] J. Y. Zhang and J. Mitroy, Phys. Rev. A **78**, 012703 (2008).
- [23] S. K. Houston and R. J. Drachman, Phys. Rev. A **3**, 1335 (1971).
- [24] M. W. J. Bromley, J. Mitroy, and G. G. Ryzhikh, J. Phys. B: At. Mol. Opt. Phys. **31**, 4449 (1998).
- [25] M. Basu and A. S. Gosh, Phys. Rev. A **43**, 4746 (1991); M. R. McAlinden, A. A. Kernoghan, and H. R. J. Walters, J. Phys. B: At. Mol. Opt. Phys. **30**, 1543 (1997).
- [26] H. Saarikoski, A. Harju, M. J. Puska, and R. M. Nieminen, Phys. Rev. Lett. **93**, 116802 (2004).
- [27] E. R. Johnson, I. D. Mackie, and G. A. DiLabio, J. Phys. Org. Chem. **22**, 1127 (2009).
- [28] A. Zubiaga, F. Tuomisto, and M. J. Puska, Phys. Rev. A **85**, 052707 (2012); A. Zubiaga and M. J. Puska, “Single particle effective potentials for Ps,” In preparation.